

1-Octanol/Water Partition Coefficients of *n*-Alkanes from Molecular Simulations of Absolute Solvation Free Energies

Nuno M. Garrido,^{†,‡} António J. Queimada,[†] Miguel Jorge,[†] Eugénia A. Macedo,[†] and Ioannis G. Economou^{*,‡}

Laboratory of Separation and Reaction Engineering (LSRE), Departamento de Engenharia Química, Faculdade de Engenharia, Universidade do Porto, Rua do Dr. Roberto Frias, 4200-465 Porto, Portugal and Molecular Thermodynamics and Modeling of Materials Laboratory, Institute of Physical Chemistry, National Center for Scientific Research “Demokritos”, GR-153 10, Aghia Paraskevi Attikis, Greece

Received April 30, 2009

Abstract: The 1-octanol/water partition coefficient is an important thermodynamic variable usually employed to understand and quantify the partitioning of solutes between aqueous and organic phases. It finds widespread use in many empirical correlations to evaluate the environmental fate of pollutants as well as in the design of pharmaceuticals. The experimental evaluation of 1-octanol/water partition coefficients is an expensive and time-consuming procedure, and thus, theoretical estimation methods are needed, particularly when a physical sample of the solute may not yet be available, such as in pharmaceutical screening. 1-Octanol/water partition coefficients can be obtained from Gibbs free energies of solvation of the solute in both the aqueous and the octanol phases. The accurate evaluation of free energy differences remains today a challenging problem in computational chemistry. In order to study the absolute solvation Gibbs free energies in 1-octanol, a solvent that can mimic many properties of important biological systems, free energy calculations for *n*-alkanes in the range C₁–C₈ were performed using molecular simulation techniques, following the thermodynamic integration approach. In the first part of this paper, we test different force fields by evaluating their performance in reproducing pure 1-octanol properties. It is concluded that all-atom force fields can provide good accuracy but at the cost of a higher computational time compared to that of the united-atom force fields. Recent versions of united-atom force fields, such as Gromos and TraPPE, provide satisfactory results and are, thus, useful alternatives to the more expensive all-atom models. In the second part of the paper, the Gibbs free energy of solvation in 1-octanol is calculated for several *n*-alkanes using three force fields to describe the solutes, namely Gromos, TraPPE, and OPLS-AA. Generally, the results obtained are in excellent agreement with the available experimental data and are of similar accuracy to commonly used QSPR models. Moreover, we have estimated the Gibbs free energy of hydration for the different compounds with the three force fields, reaching average deviations from experimental data of less than 0.2 kcal/mol for the case of the Gromos force field. Finally, we systematically compare different strategies to obtain the 1-octanol/water partition coefficient from the simulations. It is shown that a fully predictive method combining the Gromos force field in the aqueous phase and the OPLS-AA/TraPPE force field for the organic phase can give excellent predictions for *n*-alkanes up to C₈ with an absolute average deviation of 0.1 log *P* units to the experimental data.

1. Introduction

In several biochemical processes and for successful drug design strategies in the pharmaceutical industry, a correct understanding of the interactions of a given solute in both aqueous (hydrophilic) and biological (lipophilic) media is necessary.^{1–4} Together with the Gibbs free energy of solute transfer, the corresponding partition coefficient between the 1-octanol and the water phases is probably the most important input parameter used in quantitative structure–property relationships (QSPR) to correlate and predict many solute properties.⁵ Especially in the pharmaceutical industry, the prediction of drug partitioning, hydrophobicity, and even pharmacokinetic characteristics in biological systems can be quantified by expressions based on the 1-octanol/water partition coefficient^{2,3,6} (commonly known as *P* or even log *P*). Furthermore, log *P* is also used as a measure of the activity of agrochemicals, the degree of purity in metallurgy, and the hydrophobicity in environmental problems. Partition coefficient data are also useful to estimate the solubility of a solute in a solvent.^{7,8}

The partition coefficient of a solute between 1-octanol and water was first introduced in 1964 by Hansch and Fujita,⁹ and since then, many different approaches have been developed in an attempt to estimate this property. In the beginning, mostly semiempirical approaches based on the sum of fragment contributions or atom-derived group equivalents were proposed.^{1–3,10} Nowadays, fragment additive schemes remain a standard method to estimate solvation free energies and partition coefficients,¹¹ but the most common methods to estimate solvation properties are procedures based on QSPR that (cor)relate partition coefficients or solvation properties with other calculated or available molecular properties.^{12–14} Although these methods are considerably fast and applicable to large databases of molecular structures, they require large multiparameter tables having the disadvantage that whenever new molecules/compounds are under study, these need to be similar to the ones contained in the training set. This is evidenced by the lack of existing parameters to calculate log *P* for new chemical groups.^{15–17} In short, we can conclude that QSPR methods are statistically rather than physically based. Simulations based on linear response theory and molecular descriptors to derive empirical relationships for estimating log *P* values have been carried out by Duffy and Jorgensen.¹⁸ Finally, approaches based on continuum models have also been investigated.^{15,16,19}

Besides the above-mentioned estimation methods, the partition coefficient can also be obtained from experiments, by applying e.g., the shake-flask method^{20–22} for generating the saturated liquid phases, followed by sampling and quantitative solute analysis (e.g., high-performance liquid chromatography²³). Still, this can be a very expensive and time-consuming procedure, and thus, has limited practical use for product design, such as in pharmaceutical screening.

A different approach to all of the above is to use information of the free energy of solvation in water and in octanol to estimate the partition coefficient. From Gibbs free energies of solvation in two different phases at temperature *T*, one can calculate the corresponding partition coefficient, according to the following expression:

$$\log P^{1\text{-octanol/water}} = \frac{\Delta_{\text{hyd}}G - \Delta_{\text{solv}}G}{2.303RT} \quad (1)$$

where $\Delta_{\text{hyd}}G$ is the hydration free energy, and $\Delta_{\text{solv}}G$ is the Gibbs free energy of solvation in 1-octanol. The first computational approaches involving this relationship go back to the 1980s.^{24–26} Recent developments in simulation methods and increased computing power allow today the calculation of the absolute solvation free energies of complex molecules, such as amino acid analogues, directly from molecular simulations.^{27–30} Thus, we propose here an innovative approach to predict the 1-octanol/water partition coefficient without (or at least with a minimum) experimental information, based on the estimation of absolute solvation energies in water and 1-octanol, obtained from molecular simulation.

Regarding solvation, the majority of previously published studies focused on aqueous media (e.g., see a review paper by Tomasi and Persico³¹), but nowadays, computer simulations can be used to model and understand molecular-level interactions of biological membranes, proteins, and lipids. It is now possible to simulate the interactions of small solutes with complex biological membranes by explicit simulation of the lipid-bilayers,³² an approach that has the disadvantage of being very computationally expensive.³³ Therefore, alternatives are sought to mimic the fundamental characteristics of biological systems using simpler molecules. Numerous solvents, such as oils,¹ chloroform,^{5–9} or alkanes,³⁴ have been tested to study and reproduce the hydrophobic properties of organic systems, but 1-octanol remains today the most important reference solvent for this kind of study. The amphiphilic nature of the 1-octanol molecule (a polar headgroup attached to a flexible nonpolar tail) gives this molecule similar characteristics to the main constituents of lipid biomembranes. 1-octanol molecules can also mimic the complex behavior of the soil and, thus, play an important role in the prediction of solute partitioning in environmental fate and toxicological processes.³⁵ Although 1-octanol cannot form long, stable complex structures such as bilayers,³⁶ which are typical of lipid solutions, it can form liquid aggregates^{33,35} and mimic successfully many of the properties of biologically relevant systems. Consequently, it has been widely used for this purpose.

Several simulation studies related to 1-octanol systems have been reported in the literature. In the work of Debolt and Kollman,³³ pure 1-octanol and water-saturated 1-octanol physical properties were studied in detail. More recently, MacCallum and Tieleman³⁶ investigated 1-octanol mixtures at different hydration levels, including the calculation of pure 1-octanol physical properties using various force fields (FF). In that study, formation of hydrogen-bonded chains in 1-octanol/water systems were observed, which interestingly become more spherical with increasing water concentration.

* Corresponding author. E-mail: economou@chem.demokritos.gr.

[†] Laboratory of Separation and Reaction Engineering.

[‡] Molecular Thermodynamics and Modeling of Materials Laboratory.

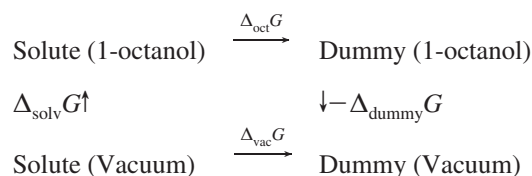
On the contrary, in pure 1-octanol these clusters are long and thin. Chen and Siepmann³⁵ identified these microscopic structural differences in the aggregate/micelle formation between dry and water-saturated 1-octanol using configurational-bias Metropolis Monte Carlo simulations in the Gibbs ensemble. Regarding free energy calculations, most studies in 1-octanol have reported only relative free energy changes, i.e., the free energy associated with a mutation from one solute into another solute of similar structure, which is a different approach than the one followed here. Studied systems include: benzene to phenol,³³ ethylbenzene to phenol, pyridine to benzene, cyclopentane to tetrahydrofuran, methanol to methylamine, iso-propanol to iso-propane, acetamide to acetone, and phenol to benzene.¹⁵ Finally, Gibbs free energies of transfer of *n*-alkanes and primary alcohols between water and (dry or wet) 1-octanol were obtained by Chen et al.³⁷

Our starting point in the present study is to evaluate/predict the Gibbs free energy of solvation of *n*-alkanes up to C₈ in 1-octanol. The availability of free energy data can be used to understand the behavior of complex systems and has the potential to revolutionize several scientific and technological fields,^{38,39} particularly in the pharmaceutical industry.⁴⁰ Solvation free energy can also be an important input parameter in order to predict solubility.^{17,41} Several investigations regarding free energy calculations in aqueous systems have been reported in the literature,^{27,28,42–47} and it is now well established that accurate results can be obtained directly from molecular simulation methods. However, simulations of solvation in nonaqueous solvents are less common. In particular, for 1-octanol, apart from the works of Chen and Siepmann,^{35,37} there is clearly a lack of a systematic study, particularly for solvation of longer alkanes. We aim here to fill this gap by presenting calculations of absolute solvation free energies of eight alkanes in 1-octanol. Initially, a comparison is made between several FF's, including all-atom (AA) and united-atom (UA) descriptions, in reproducing pure 1-octanol physical properties. Afterward, we present a comparison of three popular FF's, namely TraPPE, Gromos, and OPLS-AA, to represent solute molecules by analyzing their performance in predicting the 1-octanol absolute Gibbs free energy of solvation for *n*-alkanes up to C₈. Finally, calculation of the hydration free energies and 1-octanol/water partition coefficient by molecular simulation is discussed.

The remainder of this paper is organized as follows: in Section 2, we describe the computational methods used for the Gibbs free energy calculation, particularly the thermodynamic integration, the molecular dynamics (MD) simulation details, and the FF's tested; in Section 3.1, results for the pure 1-octanol physical properties predicted using different FF's are shown, while the capability of molecular simulation methods in predicting solvation free energies and 1-octanol/water partition coefficients are discussed in Sections 3.2–3.4. The main conclusions of this work are summarized in Section 4.

2. Computational Methods

2.1. Thermodynamic Integration. The solvation process consists of the transfer of a compound from a well-defined state (gas/vacuum) to another state (solution), and the solvation free energy may be defined as the free energy difference given by the total reversible work associated with changing the Hamiltonian of the system from the gas to the liquid state.⁴⁸ Solvation can be measured experimentally or calculated using an appropriate model and methodology. Experimental free energies are commonly estimated from solute concentration measurements in two-phase systems (vapor and liquid solution) in which, after reaching equilibrium, one evaluates the transfer of molecules between the two phases (see refs 49 and 50 for equations and details). From the theoretical point of view, in the ideal gas approximation, the interaction of a solute with its environment in the gas state is effectively zero, and only the interactions of the solute with a particular solvent environment need to be considered. Free energy is a state function and can, thus, be calculated by molecular simulation based on the construction of a thermodynamic cycle that may include nonphysical transformations necessary to make the calculation feasible. Thus, the 1-octanol solvation free energy at temperature *T* and pressure *P*, $\Delta_{\text{solv}}G(P,T)$, can be calculated using the following thermodynamic cycle:⁵¹



where $\Delta_{\text{oct}}G$ is the free energy associated with the mutation of the solute molecules into dummy molecules in a 1-octanol media, $\Delta_{\text{vac}}G$ is the free energy associated with the same process in a vacuum, and finally $\Delta_{\text{dummy}}G$ can be seen as the hypothetical solvation free energy of a dummy species. Dummy molecules do not interact with their environment. In practice, these molecules have no electrostatic or van der Waals interactions, but their intramolecular bonded interactions are the same as in the solute molecules. As a consequence, $\Delta_{\text{dummy}}G$ is equal to zero, and we can write the following equation for the thermodynamic cycle:

$$\Delta_{\text{solv}}G = \Delta_{\text{vac}}G - \Delta_{\text{oct}}G - \Delta_{\text{dummy}}G = \Delta_{\text{vac}}G - \Delta_{\text{oct}}G \quad (2)$$

The separate calculation in vacuum is necessary to compensate for changes in solute–solute intramolecular nonbonded interactions that take place when the intermolecular interactions are switched off. For each case (solvent and vacuum), the associated free energy (expressed in terms of ΔG for the NPT ensemble) is estimated here using the thermodynamic integration method,^{48,52} whose algorithm is as follows: let us consider two generic well-defined states, an initial reference state (state 0) and a final target state (state 1) with Hamiltonians \mathcal{H}_0 and \mathcal{H}_1 , respectively. A coupling parameter, λ , can be added to the Hamiltonian, $\mathcal{H}(\mathbf{p}, \mathbf{q}; \lambda)$, where \mathbf{p} is the linear momentum and \mathbf{q} the atomic position,

and used to describe the transition between the two states: $\mathcal{H}(\mathbf{p}, \mathbf{q}; 0) \rightarrow \mathcal{H}(\mathbf{p}, \mathbf{q}; 1)$. Considering several discrete and independent λ values between 0 and 1, equilibrium averages can be used to evaluate derivatives of the free energy with respect to λ . One then integrates the derivatives of the free energy along a continuous path connecting the initial and final states in order to obtain the energy difference between them:

$$\Delta G = \int_0^1 \left\langle \frac{\partial \mathcal{H}(\mathbf{p}, \mathbf{q}, \lambda)}{\partial \lambda} \right\rangle_{\lambda} d\lambda \quad (3)$$

In practice, the solvation free energy can be estimated as follows: i) simulate the system in 1-octanol at different λ values; ii) simulate the system in vacuum at different λ values; and iii) compute the solvation free energy from eq 4:

$$\Delta_{\text{solv}} G = \int_0^1 \left\langle \frac{\partial \mathcal{H}^{\text{vac}}}{\partial \lambda} \right\rangle_{\lambda} d\lambda - \int_0^1 \left\langle \frac{\partial \mathcal{H}^{\text{oct}}}{\partial \lambda} \right\rangle_{\lambda} d\lambda \quad (4)$$

Notice that because we are using thermodynamic integration, which involves equilibrium runs at independent λ values, the direction of the process is irrelevant, and the results for $\Delta_{\text{solv}} G$ are free of hysteresis. This is an important advantage relative to other methods (e.g., slow growth) where the results depend on the direction of the calculation.^{27,47}

As a final remark, one should notice that, since we are studying nonpolar solute molecules (*n*-alkanes), the only contribution to the free energy comes from the process of “turning off” the Lennard-Jones (LJ) interactions. There is no need to separately account for a Coulombic contribution (i.e., “turning off” the solute charges) to the free energy in eq 4, as is normally done for solvation of polar molecules.

2.2. Molecular Dynamics Simulations. Molecular dynamics (MD) simulations were performed with the GRO-MACS⁵³ simulation package. The integration of Newton’s equations of motion was carried out using the leapfrog dynamic algorithm⁵⁴ with a time step of 2 fs. Langevin (stochastic) dynamics⁵⁵ were used to control the temperature with a frictional constant of 1 ps^{−1} and a reference temperature of 298 K. This approach eliminates several problems that may arise from the use of conventional thermostats in free energy calculations.⁴⁴ For constant pressure simulations, the Berendsen barostat⁵⁶ with a time constant of 0.5 ps and an isothermal compressibility of 4.5×10^{-5} bar^{−1} was used to enforce pressure coupling, where the box size was scaled at every time step. The reference pressure was always set to 1 bar. Each simulation box was cubic, with periodic boundary conditions in all directions, and contained 200 1-octanol molecules. Simulations of systems with different numbers of molecules revealed this to be the optimum system size: larger systems yielded statistically similar results but at a higher computational cost, while smaller systems exhibited finite-size effects.

The initial configuration for the pure 1-octanol simulations was generated by randomly placing 200 molecules in a large cubic box. We then run an energy minimization, followed by a constant volume equilibration of 100 ps, and finally a

5 ns long NPT production stage. Two minimization procedures were employed: first, minimization was performed using the limited-memory Broyden–Fletcher–Goldfarb–Shanno (L-BFGS) algorithm of Nocedal⁵⁷ for 5 000 steps, followed by a steepest descent minimization for 500 steps. Analysis of several observables ensured that the simulations were properly equilibrated during the NPT run. Average properties were computed by discarding the time steps pertaining to the equilibration period.

To calculate solvation free energies, it is necessary to carry out several independent simulations of each solute (from methane to *n*-octane) in each solvent (1-octanol and water) for different values of the coupling parameter, as described in Section 2.1. The starting configuration for each of these simulations was obtained by immersing a solute molecule into an equilibrated box of 200 1-octanol solvent molecules or 500 water solvent molecules. The equilibrated 1-octanol box was obtained from the NPT simulations for pure 1-octanol, described above, and a similar approach was used for water. In these simulations an energy minimization was initially performed using the same protocol as for the pure liquid simulations, followed by a constant volume equilibration of 100 ps, a constant pressure equilibration of 1 ns (enough to fully equilibrate the box volume and correctly reproduce solvent density), and finally a NVT production run of 5 ns. This procedure was repeated for each of the following 16 λ values:

$$\lambda \in \{0.0, 0.05, 0.10, 0.20, 0.30, 0.40, 0.50, 0.60, 0.65, 0.70, 0.75, 0.80, 0.85, 0.90, 0.95, 1.00\}$$

where $\lambda = 0$ refers to a fully interacting solute, and $\lambda = 1$ to a noninteracting solute. We have used such a large number of intermediate λ states because in the thermodynamic integration, the accuracy of the $\Delta_{\text{solv}} G$ value depends strongly on the smoothness of the $\partial \mathcal{H} / \partial \lambda$ vs λ curve, where a smooth profile is necessary in order to minimize numerical integration errors. In the present work, the reported statistical uncertainties were obtained from block averaging,⁵⁴ and integrals were computed via the trapezoidal rule.⁵⁸ Finally, it should be noted that in the transformation process between states with different λ values, the λ dependence of the LJ potential was interpolated between the neighboring states via soft-core interactions. The soft-core expression of Beuler et al.⁵⁹ eliminates singularities in the calculation as the LJ interactions are turned off.⁶⁰ As suggested in the literature,^{27,44} the soft-core parameter used was 0.5, which is the optimized value when the power for λ in the soft-core function is 1, and the soft-core σ value used was 0.3 nm.

2.3. Force Fields. MD simulations for pure 1-octanol were performed using six different FF’s. The FF’s examined included Gromos (versions 43A2,⁶¹ 53A5,²⁹ and 53A6²⁹), OPLS-UA,^{62,63} OPLS-AA,⁶⁴ and TraPPE.^{65–67} We have decided to test three different versions of the Gromos FF since they were parametrized for different purposes, all relevant to this work. Version 43A2 was parametrized in order to reproduce only pure solvent properties. More recently, the Gromos parameter set 53A5 was optimized to reproduce thermodynamic properties of pure liquids and the solvation Gibbs free energy of amino acid analogs in

Table 1. 1-Octanol Density and Heat of Vaporization at 1 Bar from MD Simulations and Experimental Measurements^a

| FF | T (K) | | | | | | | | | |
|--------------|-----------------------------|---------|-----------------------------|---------|-----------------------------|---------|---------------------------------|---------|--------------------------|--|
| | 280 | | 340 | | 400 | | 298 | | | |
| | ρ (kg/m ³) | dev (%) | ρ (kg/m ³) | dev (%) | ρ (kg/m ³) | dev (%) | $\Delta_{\text{vap}}H$ (kJ/mol) | dev (%) | production times (hr/ns) | |
| G43A2 | 864.4 ± 0.9 | 3.4 | 822.3 ± 0.3 | 3.9 | 779.7 ± 0.7 | 5.0 | 64.4 | −10.5 | 1.09 | |
| G53A5 | 867.9 ± 0.8 | 3.8 | 827.0 ± 0.9 | 4.5 | 785.3 ± 0.6 | 5.7 | 59.5 | −17.3 | 1.09 | |
| G53A6 | 868.0 ± 0.7 | 3.8 | 827.1 ± 1.4 | 4.5 | 785.3 ± 0.8 | 5.7 | 59.5 | −17.3 | 1.09 | |
| OPLS-UA | 859.5 ± 0.7 | 2.8 | 818.8 ± 0.6 | 3.5 | 773.5 ± 0.6 | 4.1 | 72.3 | 0.4 | 1.19 | |
| OPLS-AA | 841.8 ± 0.9 | 0.7 | 781.2 ± 1.3 | −1.3 | 719.5 ± 1.2 | −3.1 | 70.7 | −1.8 | 8.00 | |
| TraPPE | 837.0 ± 0.9 | 0.08 | 793.4 ± 0.5 | 0.3 | 744.5 ± 0.8 | 0.2 | 67.0 | −6.9 | 1.15 | |
| Experimental | 836.26 ^b | | 791.39 ^b | | 742.75 ^b | | 71.98 ^c | | — | |

^a Computational production times per node (Intel Xeon at 3.0 GHz) for each FF is shown. ^b Data from refs 84–86. ^c Data from ref 72.

cyclohexane, while parameter set 53A6 was optimized to reproduce free energies in water.²⁹ The TraPPE FF was also chosen because it was optimized to provide accurate descriptions of pure liquids and vapor–liquid equilibria (VLE).^{65–67} It should be noted that, contrary to the original version of TraPPE where all bonds were fixed, bond stretching was modeled in our studies by a harmonic potential with force constants taken from CHARMM,⁶⁸ except for bonds involving hydrogen atoms that were constrained using LINCS.⁶⁹ Finally, we have tested the popular OPLS FF, which are designed to be transferrable to a wide range of organic molecules in the liquid phase. We have compared the united-atom (UA) against the all-atom (AA) FF because the former are expected to be computationally much cheaper.

In this work, the modified extended simplified point charge (MSPC/E)⁷⁰ model was used for the simulation of water. MSPC/E is an accurate FF for pure water and water–hydrocarbon thermodynamic properties, and it was chosen over other popular FF's for water. This FF also includes a polarization correction expected to improve the hydration predictions.²⁸

Several of the above FF's (in particular OPLS-AA, TraPPE, and Gromos 53A6) were also used to model the alkane molecules, solvated in either 1-octanol or water. Different combinations of solute–solvent FF's were tested in order to assess the influence of this choice on the free energy and the partition coefficient predictions. Dummy molecules were considered to be identical to real solute molecules in terms of mass, while their LJ interaction parameters were set to zero. In all cases, electrostatic interactions were calculated using the reaction field⁷¹ method with $\epsilon_{\text{rf,oct}} = 10.3$ (the dielectric constant for pure 1-octanol⁷²) or $\epsilon_{\text{rf,wat}} = 80$ (the dielectric constant for pure water⁷²). Tests performed with the more computationally demanding particle mesh Ewald method yielded similar results. The cutoff radii used were 1 nm for the electrostatic interactions, 1 nm for the short-range neighbor list, and 0.8–0.9 nm switched cutoff for the LJ interactions. It was also observed that the use of higher cutoff radii induces minimal perturbations in the absolute energy values. Overall, the simulation parameters described here were chosen so that the computational cost was minimized without sacrificing the accuracy of the calculations. Long range corrections for energy and pressure were also employed as it was concluded that they significantly improve the accuracy of the predicted solvation energies.²⁷

Detailed van der Waals parameters, point charges, bond stretching, bond angle bending and torsional force constants are provided in the Supporting Information for all compounds and FF's. Coordinate and topology files were built manually or with the help of the Molden⁷³ and PRODRG⁷⁴ software.

3. Results and Discussion

3.1. Pure 1-Octanol Physical Properties. The accuracy of different FF's for the prediction of pure 1-octanol properties was initially evaluated. The calculated 1-octanol densities over a wide temperature range from NPT MD and the heat of vaporization at 298 K are shown in Table 1. Densities were directly obtained from the GROMACS suite using the *g_energy* tool,⁵⁴ while heats of vaporization were estimated by taking the difference of enthalpy in the vapor and liquid phases:

$$\Delta_{\text{vap}}H = E_{\text{g}} - E_{\text{L}} + RT \quad (5)$$

where E_{g} is the total energy in the gas phase, and E_{L} is the total energy per mole in the liquid phase.

Based on the data reported in Table 1, one concludes that Gromos generally overestimates the 1-octanol densities, in line with previous studies of this FF,⁴⁷ and also significantly underestimates the vaporization enthalpy. As expected, version 43A2 of Gromos performed better than the other two versions because it was optimized to reproduce pure solvent liquid properties. The TraPPE FF provides excellent accuracy for the density over the temperature range but slightly underestimates the enthalpy of vaporization. Conversely, OPLS-UA overestimates the density at all temperatures but does an excellent job at predicting the enthalpy of vaporization. OPLS-AA improves significantly over OPLS-UA yielding good predictions of both density and vaporization enthalpy but at the cost of an increased computational time. In fact, computational production times, included in Table 1, show that this AA FF is more than 7 times more expensive compared to the UA approaches. One should also notice that for higher temperatures, OPLS-AA accuracy decreases. In general, an AA FF is preferable than a UA FF, provided that one can afford the additional computational cost. For simulations where minimization of computing cost is an important issue, such as in the highly demanding free energy calculations performed in this work, it is reasonable to use a UA approximation, at least for the solvent. In this case, TraPPE is probably the best option, since it performs well

Table 2. Comparison of $\Delta_{\text{vac}}G$, $\Delta_{\text{oct}}G$, and $\Delta_{\text{solv}}G$ (all in kcal/mol) Predictions for *n*-Alkanes in 1-Octanol Using TraPPE, Gromos and OPLS-AA/TraPPE FF's against Available Experimental Data at 298 K¹⁶

| solute | TraPPE | | | Gromos | | | OPLS-AA/TraPPE | | | expt |
|-------------------|------------------------|------------------------|-------------------------|------------------------|------------------------|-------------------------|------------------------|------------------------|-------------------------|-------------------------|
| | $\Delta_{\text{vac}}G$ | $\Delta_{\text{oct}}G$ | $\Delta_{\text{solv}}G$ | $\Delta_{\text{vac}}G$ | $\Delta_{\text{oct}}G$ | $\Delta_{\text{solv}}G$ | $\Delta_{\text{vac}}G$ | $\Delta_{\text{oct}}G$ | $\Delta_{\text{solv}}G$ | $\Delta_{\text{solv}}G$ |
| methane | 0 | -0.5 ± 0.2 | 0.5 ± 0.1 | 0 | -0.4 ± 0.1 | 0.4 ± 0.1 | 0 | -0.2 ± 0.1 | 0.2 ± 0.1 | 0.5 |
| ethane | 0 | 0.4 ± 0.2 | -0.4 ± 0.2 | 0 | 0.9 ± 0.2 | -0.9 ± 0.2 | 0 | 0.5 ± 0.2 | -0.5 ± 0.2 | -0.6 |
| propane | 0 | 1.0 ± 0.2 | -1.0 ± 0.2 | 0 | 1.9 ± 0.2 | -1.9 ± 0.2 | -0.6 ± 0.1 | 0.6 ± 0.2 | -1.2 ± 0.2 | -1.2^a |
| <i>n</i> -butane | 0 | 1.4 ± 0.2 | -1.4 ± 0.2 | 0.0 ± 0.1 | 2.9 ± 0.2 | -2.9 ± 0.2 | -1.3 ± 0.1 | 0.6 ± 0.2 | -1.9 ± 0.2 | -1.8^a |
| <i>n</i> -pentane | 0.1 ± 0.1 | 2.3 ± 0.2 | -2.2 ± 0.2 | -0.1 ± 0.1 | 3.3 ± 0.2 | -3.4 ± 0.2 | -2.1 ± 0.1 | 0.7 ± 0.2 | -2.8 ± 0.2 | -2.3^a |
| <i>n</i> -hexane | 0.2 ± 0.1 | 2.9 ± 0.2 | -2.7 ± 0.2 | -0.1 ± 0.1 | 4.4 ± 0.2 | -4.5 ± 0.2 | -2.9 ± 0.1 | 0.5 ± 0.2 | -3.4 ± 0.2 | -3.3 |
| <i>n</i> -heptane | 0.3 ± 0.1 | 3.5 ± 0.2 | -3.2 ± 0.2 | -0.1 ± 0.1 | 4.7 ± 0.2 | -4.8 ± 0.2 | -3.8 ± 0.1 | 0.2 ± 0.2 | -4.0 ± 0.2 | -4.1 |
| <i>n</i> -octane | 0.4 ± 0.1 | 3.7 ± 0.2 | -3.4 ± 0.2 | -0.1 ± 0.1 | 6.0 ± 0.2 | -6.1 ± 0.2 | -4.9 ± 0.2 | -0.1 ± 0.3 | -4.7 ± 0.3 | -4.6 |

^a Values estimated from eq 6.

for pure solvent liquid properties and is also able to accurately describe VLE.⁶⁵

3.2. Free Energies of Solvation in 1-octanol. The Gibbs free energy of solvation of *n*-alkanes in 1-octanol at 298 K was calculated from MD, as described above. Simulations were performed using three different FF's for the representation of both 1-octanol and *n*-alkane molecules, namely Gromos 53A6,²⁹ TraPPE,^{65–67,75–77} and OPLS-AA.⁶⁴ The 53A6 version of Gromos was preferred over the other two versions as it was parametrized to reproduce solvation properties in a polar solvent. Preliminary calculations using the OPLS-AA FF to model both alkanes and octanol showed that the computational time required for the accurate estimation of $\Delta_{\text{solv}}G$ was very high. As shown in Section 3.1, this is due to the high cost associated to an AA description of 1-octanol. Consequently, 1-octanol molecules were modeled with the TraPPE FF instead, and these calculations are referred to as OPLS-AA/TraPPE in the remainder of this paper. We have also tested a combination of OPLS-AA for the solutes with OPLS-UA for the solvent for consistency. Unfortunately, differences between experimental data and simulations from a preliminary test with propane were as high as 1 kcal/mol, and this combination of FF was not pursued further. It should be noted that deficiencies of the OPLS-UA FF in reproducing hydration free energies and hydrocarbon solubilities in water were also reported by MacCallum and Tieleman.³⁶

Thermodynamic integration was performed using the three FF's for the solutes in both vacuum and solvent medias. Representative results for the integrand of eq 4 in the octanol

phase are shown in Figure 1 based on the Gromos 53A6 FF, while similar results for all FF's are given in the Supporting Information. Furthermore, MD calculations for $\Delta_{\text{vac}}G$, $\Delta_{\text{oct}}G$ and $\Delta_{\text{solv}}G$ from the different FF's are shown in Table 2, with experimental data reported for comparison, while the different data sets for $\Delta_{\text{solv}}G$ are shown in Figure 2. It should be noted that the experimental values in Table 2 and Figure 2 represent solvation free energies of *n*-alkanes in water-saturated 1-octanol solutions, since there are no data available for anhydrous 1-octanol, which is used in the simulations. However, the difference between the free energy of solvation determined in pure and water-saturated 1-octanol is typically small, on the order of 0.2–0.4 kcal/mol¹⁶ (and refs 78–80). Moreover, for the case of propane, *n*-butane, and *n*-pentane, there are no available experimental data. To allow for a more comprehensive comparison of our simulations with experimental results, experimental values presented in Table 2 marked with *a* were estimated from

$$\Delta_{\text{solv}}G^{\text{octanol}} = \Delta_{\text{solv}}G^{\text{water}} - \log P^{\text{octanol/water}} \times 2.303 \times RT \quad (6)$$

where $\Delta_{\text{solv}}G^{\text{water}}$ are experimental data from Michielan et al.,⁸¹ and $\log P^{\text{octanol/water}}$ are the 1-octanol/water partition coefficients suggested by Sangster.³

In general, the calculated $\Delta_{\text{solv}}G$ decrease with increasing chain length is consistent with the experimental data. Calculations based on OPLS-AA/TraPPE FF provide the best agreement with experimental data, while Gromos predicts lower $\Delta_{\text{solv}}G$ values and TraPPE predicts higher $\Delta_{\text{solv}}G$ than the experiments. The average deviation between the experi-

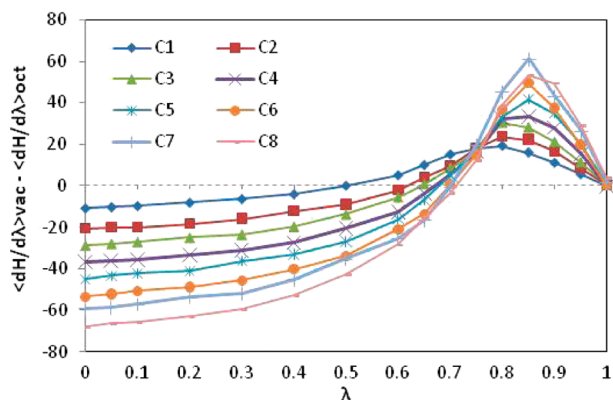
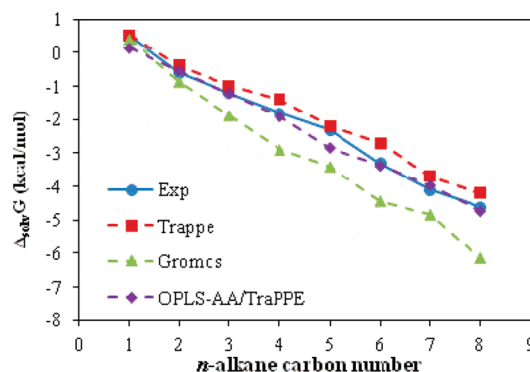
**Figure 1.** Derivative of the Hamiltonian with respect to λ as a function of λ for *n*-alkanes in 1-octanol using the Gromos FF.**Figure 2.** $\Delta_{\text{solv}}G$ for *n*-alkanes in 1-octanol at 298 K as a function of carbon number: Experimental data and MD simulations.

Table 3. $\Delta_{\text{vac}}G$, $\Delta_{\text{wat}}G$, and $\Delta_{\text{hyd}}G$ (all in kcal/mol) Predictions for *n*-alkanes in MSPC/E Water Using TraPPE, Gromos, and OPLS-AA/TraPPE FF's against Available Experimental Data^a at 298 K^{49,87}

| solute | TraPPE | | | Gromos | | | OPLS-AA/TraPPE | | | expt | simulation |
|-------------------|------------------------|------------------------|---------------------------------|------------------------|------------------------|---------------------------------|------------------------|------------------------|---------------------------------|------------------------|--------------------------------|
| | $\Delta_{\text{vac}}G$ | $\Delta_{\text{wat}}G$ | $\Delta_{\text{hyd}}G$ | $\Delta_{\text{vac}}G$ | $\Delta_{\text{wat}}G$ | $\Delta_{\text{hyd}}G$ | $\Delta_{\text{vac}}G$ | $\Delta_{\text{wat}}G$ | $\Delta_{\text{hyd}}G$ | $\Delta_{\text{hyd}}G$ | $\Delta_{\text{hyd}}G$ |
| methane | 0 | -2.3 ± 0.1 | 2.3 ± 0.1 | 0 | -2.0 ± 0.1 | 2.0 ± 0.1 | 0 | -2.4 ± 0.1 | 2.4 ± 0.1 | 1.98 | 2.0–2.6 ^{27,28,42–47} |
| ethane | 0 | -2.1 ± 0.1 | 2.1 ± 0.1 | 0 | -1.8 ± 0.1 | 1.8 ± 0.1 | 0 | -2.6 ± 0.1 | 2.6 ± 0.1 | 1.81 | 1.7–2.6 ^{42,43,46,47} |
| propane | 0 | -2.4 ± 0.1 | 2.4 ± 0.1 | 0 | -1.9 ± 0.1 | 1.9 ± 0.1 | -0.6 ± 0.1 | -3.7 ± 0.1 | 3.1 ± 0.1 | 2.02 | 1.9–2.7 ^{27,28,42–47} |
| <i>n</i> -butane | 0 | -2.8 ± 0.1 | 2.8 ± 0.1 | -0.0 ± 0.1 | -1.7 ± 0.2 | 1.7 ± 0.2 | -1.3 ± 0.1 | -4.7 ± 0.2 | 3.4 ± 0.2 | 2.18 | 1.9–3.5 ^{27,28,42–47} |
| <i>n</i> -pentane | 0.1 ± 0.1 | -3.0 ± 0.1 | 3.1 ± 0.1 | -0.1 ± 0.1 | -2.1 ± 0.2 | 2.0 ± 0.2 | -2.1 ± 0.1 | -5.6 ± 0.2 | 3.5 ± 0.2 | 2.36 | 2.7–3.7 ^{42,47} |
| <i>n</i> -hexane | 0.2 ± 0.1 | -3.2 ± 0.1 | 3.4 ± 0.1 | -0.1 ± 0.1 | -2.3 ± 0.2 | 2.2 ± 0.2 | -2.9 ± 0.1 | -7.1 ± 0.2 | 4.2 ± 0.2 | 2.58 | n.a. |
| <i>n</i> -heptane | 0.3 ± 0.1 | -3.5 ± 0.1 | 3.7 ± 0.1 | -0.1 ± 0.1 | -2.4 ± 0.2 | 2.3 ± 0.2 | -3.8 ± 0.1 | -7.9 ± 0.2 | 4.2 ± 0.2 | 2.65 | n.a. |
| <i>n</i> -octane | 0.4 ± 0.1 | -3.8 ± 0.2 | 4.2 ± 0.2 | -0.1 ± 0.1 | -2.4 ± 0.2 | 2.3 ± 0.2 | -4.9 ± 0.2 | -9.7 ± 0.2 | 4.8 ± 0.2 | 2.93 | n.a. |

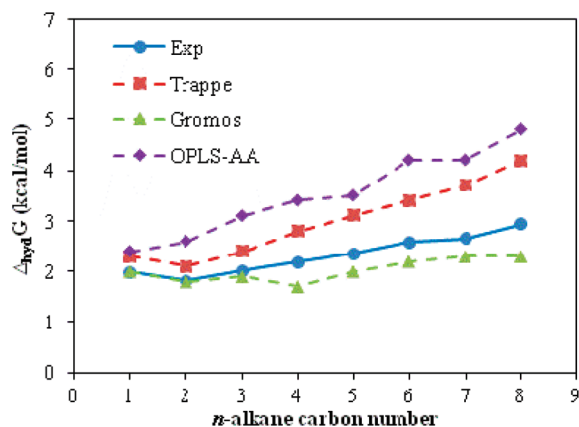
^a For comparison, literature values based on molecular simulation are included.

mental data and the simulations is 0.1 kcal/mol for OPLS-AA/TraPPE, 0.8 kcal/mol for Gromos, and 0.4 kcal/mol for TraPPE. In the pharmaceutical industry, accuracies of 0.5–1.0 kcal/mol are required for predicting affinities in drug binding.⁴³ In this respect, the polarizable continuum model MST, originally developed by Miertus et al.,⁸² was recently reparameterized¹⁶ for reproducing solvation free energies in 1-octanol, and differences of 0.4–0.6 kcal/mol were observed for *n*-alkanes from C₆–C₈. Even more, this (re)parametrization required the knowledge of the solvation experimental data, which for complex molecules is a clear disadvantage. Indeed, the methodology used in this work can provide molecular level details and insights that cannot be obtained using continuous models, since solvent molecules are modeled explicitly. The average absolute deviation (AAD) observed in this work for the organic phase are considerably smaller than the typical AAD published in the literature for aqueous systems (see Section 3.3).

In short, the accuracy of the OPLS-AA/TraPPE combination of FF's for solute/solvent to describe the Gibbs energy of solvation in 1-octanol is clearly better in comparison with other published studies. These calculations also verify that an AA description of the solute molecules improves the accuracy in the prediction of solvation energies.

3.3. Free Energies of Hydration of *n*-Alkanes. Contrary to the case of 1-octanol, there are many experimental data and simulation studies available in the literature concerning $\Delta_{\text{hyd}}G$ of *n*-alkanes. In Table 3, a compilation of such data is presented (last two columns). In our simulations, the same molecular models as above were used for *n*-alkanes. Simulation results for $\Delta_{\text{vac}}G$, $\Delta_{\text{wat}}G$, and $\Delta_{\text{hyd}}G$ from the various FF's are presented in Table 3. A graphical comparison of simulation results with experimental data for $\Delta_{\text{hyd}}G$ is shown in Figure 3. We can observe that, while in 1-octanol solvation free energies are negative and decrease with the chain length so that the solubility in octanol increases, the opposite is found in water, and the solubility decreases with the chain length. These facts are supported both by experiments and simulation.

For the hydration calculations, the deviation between experimental data and our MD results is larger than in the case of 1-octanol, although in the same accuracy range of previously published studies for these systems.^{27,28,44,45,47} Typical average absolute deviations for hydration Gibbs free energy calculations available in the literature range from 0.8 to 1.5 kcal/mol, as can be found in the study of Shirts

**Figure 3.** $\Delta_{\text{hyd}}G$ for *n*-alkanes at 298 K as a function of carbon number: Experimental data and MD simulations.

et al.²⁷ for 15 amino acid side chain analogs: 1.2 kcal/mol for AMBER, 1.1 kcal/mol for CHARMM, and 0.8 kcal/mol for OPLS-AA. Furthermore, for the hydration of alkanes (up to C₅), average deviations of 0.5 kcal/mol were reported.^{42,43,46,47}

Gromos provides the best agreement with the experimental data with an AAD lower than 0.3 kcal/mol, while OPLS-AA/TraPPE predictions deviate by an average of 1.2 kcal/mol, and TraPPE by an average of 0.6 kcal/mol from the experimental data. This good performance of the Gromos FF is to be expected a priori since this FF was parametrized to reproduce free energies of hydration. Interestingly, the use of an AA description of the solute in hydration free energy calculations seems to be less important than the optimization of the interaction parameters. This is in marked contrast to the case of solvation free energies in 1-octanol, as described above. Thus, it appears that it is important to take hydration free energies into consideration during the parametrization of a FF, if accurate predictions of this property are desired. Previous simulation studies have also revealed the importance of the FF used for water in the description of the hydration free energy.^{28,45}

3.4. 1-Octanol/Water Partition Coefficients. The 1-octanol/water partition coefficient at 298 K for the various *n*-alkanes can be readily estimated from eq 1 using the Gibbs free energies of solvation calculated from our MD simulations. In Table 4, simulation predictions are shown for the different FF's employed together with literature experimental data for comparison.

The overall AAD between the experimental data and the simulation results for log *P* is equal to 0.4 (in log *P* units)

Table 4. Experimental data^{2,3,88} and Simulation Predictions for the Logarithm of 1-Octanol/Water Partition Coefficient ($\log P$) using Different FF Combinations^a

| solute | $\log P$ | | | | expt |
|-------------------|----------|--------|----------------|-------------------------|------|
| | Gromos | TraPPE | OPLS-AA/TraPPE | Gromos + OPLS-AA/TraPPE | |
| methane | 1.2 | 1.3 | 1.6 | 1.3 | 1.1 |
| ethane | 2.0 | 1.8 | 2.3 | 1.7 | 1.8 |
| propane | 2.8 | 2.5 | 3.2 | 2.3 | 2.4 |
| <i>n</i> -butane | 3.4 | 3.1 | 3.8 | 2.6 | 2.9 |
| <i>n</i> -pentane | 4.0 | 3.9 | 4.6 | 3.5 | 3.4 |
| <i>n</i> -hexane | 4.9 | 4.3 | 5.6 | 4.1 | 3.9 |
| <i>n</i> -heptane | 5.2 | 5.1 | 6.0 | 4.6 | 4.7 |
| <i>n</i> -octane | 6.2 | 5.6 | 7.0 | 5.1 | 5.2 |
| AAD | 0.4 | 0.3 | 0.9 | 0.1 | — |

^a The AAD's between experiment and simulation are also included.

for Gromos, 0.3 for TraPPE and 0.9 for OPLS-AA/TraPPE. Interestingly, the TraPPE FF provides accurate $\log P$ predictions, while the corresponding solvation energies are not so accurately estimated; this can be attributed to cancellation of errors between the two phases — the high overestimation of the hydration free energy (Figure 3) is partially compensated by an overestimation of the octanol solvation free energy (Figure 2). A similar effect occurs in the Gromos predictions but from the opposite direction — underestimation of both water and octanol free energies. On the other hand, the OPLS-AA/TraPPE FF combination is much more accurate in the organic phase than in the aqueous phase, leading to larger deviations in $\log P$.

However, if one calculates $\log P$ using the most accurate simulation predictions for both $\Delta_{\text{hyd}}G$ (from Gromos) and $\Delta_{\text{solv}}G$ (from OPLS-AA/TraPPE), then an AAD of 0.14 is obtained. Clearly, this approach provides a very accurate prediction within the experimental uncertainty. Comparing accuracies of different methods can be merely qualitative, since the method performance is highly dependent on the validation set used, which may vary on size, complexity, or the overlap of information used in the training set/model correlation. Even so, similar calculations using a continuous model resulted in an AAD of 0.75 $\log P$ units,¹⁶ verifying that our predictions should be considered very satisfactory. Another published work⁸³ reports deviations of 0.6 $\log P$ units using a continuum method based on a continuous electrostatic model using atomic point charges combined with a nonelectrostatic term function of surface tension for a set of 2 116 molecules.

A final remark should be made regarding the accuracy of the available experimental data. As previously explained, $\log P$ and Gibbs free energy of solvation data are estimated following different experimental methodologies. At the same time, eq 1 provides a means to check the consistency between different data. A compilation of different data results in deviations of up to 0.8 $\log P$ units with an AAD of 0.24 $\log P$ units.

4. Conclusions

In order to predict the partition coefficient of a solute between 1-octanol and water, absolute free energy calculations were performed in 1-octanol and water solvents for different *n*-alkanes up to *n*-octane using MD and thermodynamic integration. The absolute free energies of solvation were

estimated by fully decoupling the solute from the solvent, which must be distinguished from previous studies where the relative free energies were calculated from mutations between two solutes. The method we used here is more flexible and not limited to mutations between similar structures. However, this complete decoupling requires large changes in the Hamiltonian, and potentially higher errors are introduced in the calculations as more intermediate states are required. It is also worthwhile to notice that, contrary to many other methodologies presented in the literature, we do not need the knowledge of the experimental solvation data in advance, which is a clear advantage.

Our method is capable of predicting solvation free energies of nonpolar solutes such as *n*-alkanes in 1-octanol with good accuracy. A comparison between different FF's permitted to conclude that the OPLS-AA FF for the solute in combination with the TraPPE FF for 1-octanol produces the most accurate results with differences to experimental data of 0.1 kcal/mol, which is approximately the precision of the experimental methods. The results are much improved by using an AA model for the *n*-alkanes, relative to UA models, with very little increase in computational cost. Arguably, the predictions could be further improved by adopting an AA description of the 1-octanol solvent as well, since this yielded a better representation of pure liquid properties. However, the associated high computational cost currently precludes this approach.

Moreover, we reproduced experimental hydration free energies of the same *n*-alkanes with average deviations of 0.3 kcal/mol, using the Gromos FF. For hydration free energies, a correct parametrization of the interaction potentials seems to be more important than using an AA description of the solute. For this reason, Gromos, which included hydration free energies in its parametrization, performed better than OPLS-AA.

Combining the simulated values of solvation free energy of the *n*-alkanes in water and 1-octanol, we were able to predict the corresponding partition coefficients with an accuracy that is within the experimental uncertainty. All FF combinations that were tested here performed well, in some cases due to the cancellation of errors in both solvation free energies. The most accurate $\log P$ predictions are afforded by the combination of the Gromos FF in the water phase with the OPLS-AA/TraPPE FF in the organic phase, reaching

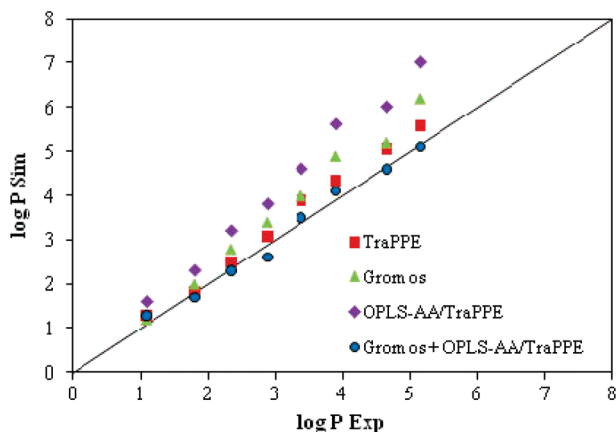


Figure 4. Comparison of $\log P$ predictions using different FF's against experimental data.

absolute deviations to experimental data of 0.1 $\log P$ units, which can be comparable to the widely used QSPR statistical methods.

Acknowledgment. The authors are grateful for the support provided by Fundação para a Ciência e a Tecnologia (FCT) Portugal, through projects FEDER/POCI/2010 and REEQ/1164/EQU/2005. N.M.G. acknowledges his FCT Ph.D. scholarship SFRH/BD/47822/2007 and financial support for his visit to NCSR “Demokritos”. Financial support from the Greek Secretariat of Research and Technology was provided for N.M.G. to stay in NCSR “Demokritos”. A.J.Q. acknowledges financial support from POCI/N010/2006, and M.J. acknowledges financial support from Ciência 2008.

Supporting Information Available: Detailed van der Waals parameters, point charges, bond stretching, bond angle bending and torsional force constants are provided for all compounds and FF. Detailed bonded and nonbonded potential parameters for all the compounds and for the different FF under study as well as plots of the derivatives of the Hamiltonian with respect to the coupling parameter for all the case studies are available. This material is available free of charge via the Internet at <http://pubs.acs.org>.

References

- Leo, A.; Hansch, C.; Elkins, D. Partition Coefficients and Their Uses. *Chem. Rev.* **1971**, *71* (6), 525–616.
- Hansch, C.; Leo, A.; Hoekman, D. *Exploring QSAR: Hydrophobic, Electronic and Steric Constants*. American Chemical Society: Washington, DC, 1995.
- Sangster, J. *Octanol-Water Partitioning Coefficients: Fundamentals and Physical Chemistry*. John Wiley & Sons: Chichester, U.K., 1997.
- Perlovich, G. L.; Kurkov, S. V.; Kinchin, A. N.; Bauer-Brandl, A. Solvation and Hydration Characteristics of Ibuprofen and Acetylsalicylic Acid. *AAPS PharmSciTech* **2004**, *6* (1), 1–9.
- Hansch, C.; Leo, A.; Hoekman, D. *Exploring QSAR: Fundamentals and Applications in Chemistry and Biology*. American Chemical Society: Washington DC, 1995.
- Betageri, G. V.; Rogers, J. A. Correlation of Partitioning of Nitroimidazoles in the Normal Octanol Saline and Liposome Systems with Pharmacokinetic Parameters and Quantitative Structure Activity Relationships (QSAR). *Pharmaceut. Res.* **1989**, *6* (5), 399–403.
- Yalkowsky, S. H. *Solubility and Solubilization in Aqueous Media*. Oxford University: Oxford, U.K., 1999.
- Pinho, S. P.; Macedo, E. A. Solubility in Food, Pharmaceuticals, and Cosmetic Industries. In *Developments and Applications in Solubility*, Letcher, T. M., Ed. Royal Society of Chemistry: Cambridge, U.K., 2003; pp 309–326.
- Hansch, C.; Fujita, T. ρ - π - σ analysis. A Method for the Correlation of Biological Activity and Chemical Structure. *J. Am. Chem. Soc.* **1964**, *86* (8), 1616–1626.
- Leo, A. J. Calculating $\log P$ (Oct) from Structures. *Chem. Rev.* **1993**, *93* (4), 1281–1306.
- Viswanadhan, V. N.; Ghose, A. K.; Singh, U. C.; Wendoloski, J. J. Prediction of Solvation Free energies of Small organic Molecules: Additive-constitutive models based on molecular fingerprints and atomic constants. *J. Chem. Inf. Comput. Sci.* **1999**, *39* (2), 405–412.
- Bodor, N.; Buchwald, P. Molecular Size Based Approach to Estimate Partition Properties for Organic Solutes. *J. Phys. Chem. B* **1997**, *101* (17), 3404–3412.
- Kamlet, M. J.; Doherty, R. M.; Abraham, M. H.; Marcus, Y.; Taft, R. W. Linear Solvation Energy Relationships 46: An Improved Equation for Correlation and Prediction of Octanol Water Partition Coefficients of Organic Nonelectrolytes (Including Strong Hydrogen-Bond Donor Solutes). *J. Phys. Chem.* **1988**, *92* (18), 5244–5255.
- Karelson, M. *Molecular Descriptors in QSAR/QSPR*. Wiley Interscience: New York, 2000.
- Best, S. A.; Merz, K. M.; Reynolds, C. H. Free Energy Perturbation Study of Octanol/Water Partition Coefficients: Comparison with Continuum GB/SA Calculations. *J. Phys. Chem. B* **1999**, *103* (4), 714–726.
- Curutchet, C.; Orozco, M.; Luque, F. J. Solvation in Octanol: Parametrization of the Continuum MST Model. *J. Comput. Chem.* **2001**, *22* (11), 1180–1193.
- Westergren, J.; Lindfors, L.; Hoglund, T.; Luder, K.; Nordholm, S.; Kjellander, R. In Silico Prediction of Drug Solubility: 1. Free Energy of Hydration. *J. Phys. Chem. B* **2007**, *111* (7), 1872–1882.
- Duffy, E. M.; Jorgensen, W. L. Prediction of Properties from Simulations: Free Energies of Solvation in Hexadecane, Octanol, and Water. *J. Am. Chem. Soc.* **2000**, *122* (12), 2878–2888.
- Orozco, M.; Luque, F. J. Theoretical Methods for the Description of the Solvent Effect in Biomolecular Systems. *Chem. Rev.* **2000**, *100* (11), 4187–4225.
- Bergstrom, C. A. S.; Norinder, U.; Luthman, K.; Artursson, P. Experimental and Computational Screening Models for Prediction of Aqueous Drug Solubility. *Pharmaceut. Res.* **2002**, *19* (2), 182–188.
- Glomme, A.; Marz, J.; Dressman, J. B. Comparison of a Miniaturized Shake-Flask Solubility Method with Automated Potentiometric Acid/Base Titrations and Calculated Solubilities. *J. Pharm. Sci.* **2005**, *94* (1), 1–16.
- Loftsson, T.; Hreinsdottir, D. Determination of Aqueous Solubility by Heating and Equilibration: A technical Note. *AAPS PharmSciTech* **2006**, *7* (1), E1–E4.
- Chen, X. Q.; Venkatesh, S. Miniature Device for Aqueous and Non-aqueous Solubility Measurements during Drug Discovery. *Pharmaceut. Res.* **2004**, *21* (10), 1758–1761.

- (24) Jorgensen, W.; Briggs, J.; Contreras, M. Relative Partition Coefficients for Organic Solutes from Fluid Simulations. *J. Phys. Chem.* **1990**, *94*, 1683–1686.
- (25) Essex, J. W.; Reynolds, C. A.; Richards, W. G. Relative Partition Coefficients from Partition Functions: A Theoretical Approach to Drug Transport. *Chem. Commun.* **1989**, (16), 1152–1154.
- (26) Jorgensen, W. Free Energy Calculations: A Breakthrough for Modeling Organic Chemistry in Solution. *Acc. Chem. Res.* **1989**, *22*, 184–189.
- (27) Shirts, M. R.; Pitera, J. W.; Swope, W. C.; Pande, V. S. Extremely Precise Free Energy Calculations of Amino Acid Side Chain Analogs: Comparison of Common Molecular Mechanics Force Fields for Proteins. *J. Chem. Phys.* **2003**, *119* (11), 5740–5761.
- (28) Hess, B.; van der Vegt, N. F. A. Hydration Thermodynamic Properties of Amino Acid Analogues: A Systematic Comparison of Biomolecular Force Fields and Water Models. *J. Phys. Chem. B* **2006**, *110* (35), 17616–17626.
- (29) Oostenbrink, C.; Villa, A.; Mark, A. E.; Van Gunsteren, W. F. A Biomolecular Force Field Based on the Free Enthalpy of Hydration and Solvation: The GROMOS ForceField Parameter sets 53A5 and 53A6. *J. Comput. Chem.* **2004**, *25* (13), 1656–1676.
- (30) Shivakumar, D.; Deng, Y.; Roux, B. Computations of Absolute Solvation Free Energies of Small Molecules Using Explicit and Implicit Solvent Model. *J. Chem. Theory Comput.* **2009**, *5* (4), 919–930.
- (31) Tomasi, J.; Persico, M. Molecular Interactions in Solution – an Overview of Methods Based on Continuous Distributions of the Solvent. *Chem. Rev.* **1994**, *94* (7), 2027–2094.
- (32) Tieleman, D. P.; Marrink, S. J.; Berendsen, H. J. C. A Computer Perspective of Membranes: Molecular Dynamics Studies of Lipid Bilayer Systems. *Biochim. Biophys. Acta, Rev. Biomembr.* **1997**, *1331* (3), 235–270.
- (33) Debolt, S. E.; Kollman, P. A. Investigation of Structure, Dynamics and Solvation in 1-Octanol and its Water-Saturated Solution: Molecular Dynamics and Free-Energy Perturbation Studies. *J. Am. Chem. Soc.* **1995**, *117* (19), 5316–5340.
- (34) Shih, P.; Pedersen, L. G.; Gibbs, P. R.; Wolfenden, R. Hydrophobicities of the Nucleic Acid Bases: Distribution Coefficients from Water to Cyclohexane. *J. Mol. Biol.* **1998**, *280* (3), 421–430.
- (35) Chen, B.; Siepmann, J. I. Microscopic Structure and Solvation in Dry and Wet Octanol. *J. Phys. Chem. B* **2006**, *110* (8), 3555–3563.
- (36) MacCallum, J. L.; Tieleman, D. P. Structures of Neat and Hydrated 1-Octanol from Computer Simulations. *J. Am. Chem. Soc.* **2002**, *124* (50), 15085–15093.
- (37) Chen, B.; Siepmann, J. I. Partitioning of Alkane and Alcohol Solutes between Water and (Dry or Wet) 1-Octanol. *J. Am. Chem. Soc.* **2000**, *122* (27), 6464–6467.
- (38) Kollman, P. Free Energy Calculations – Applications to Chemical and Biochemical Phenomena. *Chem. Rev.* **1993**, *93* (7), 2395–2417.
- (39) Kollman, P. A. Advances and Continuing Challenges in Achieving Realistic and Predictive Simulations of the Properties of Organic and Biological Molecules. *Acc. Chem. Res.* **1996**, *29* (10), 461–469.
- (40) Jorgensen, W. L. The Many Roles of Computation in Drug Discovery. *Science* **2004**, *303* (5665), 1813–1818.
- (41) Palmer, D. S.; Llinas, A.; Morao, I.; Day, G. M.; Goodman, J. M.; Glen, R. C.; Mitchell, J. B. O. Predicting Intrinsic Aqueous Solubility by a Thermodynamic Cycle. *Mol. Pharmacol.* **2008**, *5* (2), 266–279.
- (42) Ashbaugh, H. S.; Kaler, E. W.; Paulaitis, M. E. Hydration and Conformational Equilibria of Simple Hydrophobic and Amphiphilic Solutes. *Biophys. J.* **1998**, *75* (2), 755–768.
- (43) Kaminski, G.; Duffy, E. M.; Matsui, T.; Jorgensen, W. L. Free Energies of Hydration and Pure Liquid Properties of Hydrocarbons from the OPLS All-Atom Model. *J. Phys. Chem.* **1994**, *98*, 13077–13082.
- (44) Mobley, D. L.; Dumont, E.; Chodera, J. D.; Dill, K. A. Comparison of Charge Models for Fixed-Charge Force Fields: Small-molecule Hydration Free Energies in Explicit Solvent. *J. Phys. Chem. B* **2007**, *111* (9), 2242–2254.
- (45) Shirts, M. R.; Pande, V. S. Solvation Free Energies of Amino Acid Side Chain Analogs for Common Molecular Mechanics Water Models. *J. Chem. Phys.* **2005**, *122* (13), 134508.
- (46) Slusher, J. T. Accurate Estimates of Infinite-dilution Chemical Potentials of Small Hydrocarbons in Water via Molecular Dynamics Simulation. *J. Phys. Chem. B* **1999**, *103* (29), 6075–6079.
- (47) Wescott, J. T.; Fisher, L. R.; Hanna, S. Use of Thermodynamic Integration to Calculate the Hydration Free Energies of n-alkanes. *J. Chem. Phys.* **2002**, *116* (6), 2361–2369.
- (48) Christophe Chipot; Pohorille, A. *Free Energy Calculations - Theory and Applications in Chemistry and Biology*. Springer: Berlin, Germany, 2007.
- (49) Wolfenden, R.; Andersson, L.; Cullis, P. M.; Southgate, C. C. B. Affinities of Amino Acid Side Chains for Solvent Water. *Biochemistry* **1981**, *20* (4), 849–855.
- (50) Ben-Naim, A.; Marcus, Y. Solvation Thermodynamics of Non-ionic Solutes. *J. Chem. Phys.* **1984**, *81* (4), 2016–2027.
- (51) Leach, A. , *Molecular Modeling: Principles and Applications*. Prentice-Hall: 2001.
- (52) Kirkwood, J. G. Statistical Mechanics of Pure Fluids. *J. Chem. Phys.* **1935**, *3*, 300–313.
- (53) Van der Spoel, D.; Lindahl, E.; Hess, B.; Groenhof, G.; Mark, A. E.; Berendsen, H. J. C. GROMACS: Fast, Flexible, and Free. *J. Comput. Chem.* **2005**, *26* (16), 1701–1718.
- (54) Spoel, D. L., E.; Hess, B.; Buuren, A.; Apol, E.; Meulen-hof, P.; Tieleman, D.; Sijbers, A.; Feenstra, K.; Drunen, R.; Berendsen, H. *Gromacs User Manual - version 3.3*. The Netherlands, 2006.
- (55) van Gunsteren, W. F.; Berendsen, H. J. C. A Leap-frog Algorithm for Stochastic Dynamics. *Molec Sim.* **1988**, *1* (3), 173–185.
- (56) Berendsen, H. J. C.; Postma, J. P. M.; Vangunsteren, W. F.; Dinola, A.; Haak, J. R. Molecular Dynamics with Coupling to an External Bath. *J. Chem. Phys.* **1984**, *81* (8), 3684–3690.
- (57) Liu, D. C.; Nocedal, J. On the Limited Memory BFGS Method for Large Scale Optimization. *Math. Program.* **1989**, *45* (3), 503–528.
- (58) Chapra, S.; Canale, R. *Numerical Methods for Engineers*, 5th ed.; McGraw-Hill: New York, USA, 2006.
- (59) Beuler, T., M. R.; van Schaik, R. C.; Gerber, P. R.; van Gunsteren, W. F. Avoiding Singularities and Numerical Instabilities in Free Energy Calculations based on Molecular Simulations. *Chem. Phys. Lett.* **1994**, *222*, 529–539.

- (60) Pitera, J. W.; Van Gunsteren, W. F. A Comparison of Non-bonded Scaling Approaches for Free Energy Calculations. *Mol. Simul.* **2002**, 28 (1–2), 45–65.
- (61) van Gunsteren, W. F.; Billeter, S. R.; Eising, A. A.; Hünenberger, P. H.; Krüger, P.; Mark, A. E.; Scott, W. R. P.; Tironi, I. G. *Biomolecular Simulation: GROMOS96 Manual and User Guide*; Vdf Hochschulverlag AG an der ETH Zürich: Zürich, Switzerland, 1996.
- (62) Jorgensen, W. L. Optimized Intermolecular Potential Functions for Liquid Alcohols. *J. Phys. Chem.* **1986**, 90 (7), 1276–1284.
- (63) Jorgensen, W. L.; Madura, J. D.; Swenson, C. J. Optimized Intermolecular Potential Functions for Liquid Hydrocarbons. *J. Am. Chem. Soc.* **1984**, 106 (22), 6638–6646.
- (64) Jorgensen, W. L.; Maxwell, D. S.; Tirado-Rives, J. Development and Testing of the OPLS All-atom Force Field on Conformational Energetics and Properties of Organic Liquids. *J. Am. Chem. Soc.* **1996**, 118 (45), 11225–11236.
- (65) Chen, B.; Potoff, J. J.; Siepmann, J. I. Monte Carlo Calculations for Alcohols and their Mixtures with Alkanes. Transferable Potentials for Phase Equilibria. 5. United-atom description of Primary, Secondary, and Tertiary Alcohols. *J. Phys. Chem. B* **2001**, 105 (15), 3093–3104.
- (66) Martin, M. G.; Siepmann, J. I. Transferable Potentials for Phase Equilibria. 1. United-atom description of n-Alkanes. *J. Phys. Chem. B* **1998**, 102 (14), 2569–2577.
- (67) Martin, M. G.; Siepmann, J. I. Novel Configurational-bias Monte Carlo Method for Branched Molecules. Transferable Potentials for Phase Equilibria. 2. United-atom description of Branched Alkanes. *J. Phys. Chem. B* **1999**, 103 (21), 4508–4517.
- (68) Brooks, B. R.; Bruccoleri, R. E.; Olafson, D. J.; States, D. J.; Swaminathan, S.; Karplus, M. CHARMM: A Program for Macromolecular Energy, Minimization, and Dynamics Calculations. *J. Comput. Chem.* **1983**, 4, 187–217.
- (69) Hess, B.; Bekker, H.; Berendsen, H. J. C.; Fraaije, J. LINCS: A Linear Constraint Solver for Molecular Simulations. *J. Comput. Chem.* **1997**, 18 (12), 1463–1472.
- (70) Boulougouris, G. C.; Economou, I. G.; Theodorou, D. N. Engineering a Molecular Model for Water Phase Equilibrium over a Wide Temperature Range. *J. Phys. Chem. B* **1998**, 102 (6), 1029–1035.
- (71) Lee, F. S.; Warshel, A. A Local Reaction Field Method for Fast Evaluation of Long-range Electrostatic Interactions in Molecular Simulations. *J. Chem. Phys.* **1992**, 97 (5), 3100–3107.
- (72) Lide, D. R. *CRC Handbook of Chemistry and Physics*, 85 ed.; CRC Press: Boca Raton, FL, 2005.
- (73) Schaftenaar, G.; Noordik, J. H. Molden: a Pre- and Post-processing Program for Molecular and Electronic Structures. *J. Comput.-Aided Mol. Des.* **2000**, 14 (2), 123–134.
- (74) Schuettelkopf, A. W.; Aalten, D. M. F. v., PRODRG - a Tool for High-throughput Crystallography of Protein-ligand Complexes. *Acta Cryst. D* **2004**, 60, 1355–1363.
- (75) Stubbs, J. M.; Potoff, J. J.; Siepmann, J. I. Transferable Potentials for Phase Equilibria. 6. United-atom description for Ethers, Glycols, Ketones, and Aldehydes. *J. Phys. Chem. B* **2004**, 108 (45), 17596–17605.
- (76) Wick, C. D.; Martin, M. G.; Siepmann, J. I. Transferable Potentials for Phase Equilibria. 4. United-atom description of Linear and Branched Alkenes and Alkylbenzenes. *J. Phys. Chem. B* **2000**, 104 (33), 8008–8016.
- (77) Wick, C. D.; Stubbs, J. M.; Rai, N.; Siepmann, J. I. Transferable Potentials for Phase Equilibria. 7. Primary, Secondary, and Tertiary Amines, Nitroalkanes and Nitrobenzene, Nitriles, Amides, Pyridine, and Pyrimidine. *J. Phys. Chem. B* **2005**, 109 (40), 18974–18982.
- (78) Bernazzani, L.; Cabani, S.; Conti, G.; Mollica, V. Thermodynamic Study of the Partitioning of Organic Compounds between Water and Octan-1-ol. *J. Chem. Soc., Faraday Trans.* **1995**, 91 (4), 649–655.
- (79) Berti, P.; Cabani, S.; Conti, G.; Mollica, V. Thermodynamic Study of Organic Compounds in Octan-1-ol: Processes of Transfer from Gas to and from Dilute Aqueous Solution. *J. Chem. Soc., Faraday Trans. 1* **1986**, 82, 2547–2556.
- (80) Dallas, A. J.; Carr, P. W. A Thermodynamic and Solvatochromic Investigation of the Effect of Water on the Phase Transfer Properties of Octan-1-ol. *J. Chem. Soc., Perkin Trans. 2* **1992**, (12), 2155–2161.
- (81) Michielan, L.; Bacilieri, M.; Kaseda, C.; Moro, S. Prediction of the Aqueous Solvation Free Energy of Organic Compounds by Using Autocorrelation of Molecular Electrostatic Potential Surface Properties Combined with Response Surface Analysis. *Bioorg. Med. Chem.* **2008**, 16 (10), 5733–5742.
- (82) Miertus, S.; Scrocco, E.; Tomasi, J. Electrostatic Interaction of a Solute with a Continuum: a Direct Utilization of Ab-initio Molecular Potentials for the Prediction of Solvent Effects. *Chem. Phys.* **1981**, 55 (1), 117–129.
- (83) Bordner, A. J.; Civasotto, C. N.; Abagyan, R. A. Accurate transferable model for water, n-octanol, and n-hexadecane solvation free energies. *J. Phys. Chem. B* **2002**, 106 (42), 11009–11015.
- (84) Daubert, T.; Danner, R. *Physical and Thermodynamic Properties of Pure Chemicals: Data Compilation, version 4.1.1*; Hemisphere: New York, 2003.
- (85) Hales, J. L.; Ellender, J. H. Liquid Densities from 293 to 490 K of 9 Aliphatic Alcohols. *J. Chem. Thermodyn.* **1976**, 8 (12), 1177–1184.
- (86) Smith, B. D.; Srivastava, R. *Thermodynamic Data for Pure Compounds. Part B. Halogenated Hydrocarbons and Alcohols*; Elsevier: Amsterdam, The Netherlands, 1986.
- (87) Cabani, S.; Gianni, P.; Mollica, V.; Lepori, L. Group Contributions to the Thermodynamic Properties of Non-Ionic Organic Solutes in Dilute Aqueous Solution. *J. Solut. Chem.* **1981**, 10 (8), 563–595.
- (88) Rytting, E.; Lentz, K. A.; Chen, X. Q.; Qian, F.; Venkatesh, S. Aqueous and cosolvent solubility data for drug-like organic compounds. *AAPS J.* **2005**, 7 (1), E78–E105.

CT900214Y